ISBN: 978-3-95450-184-7 doi:10.18429/JACoW-IPAC2018-THPAL015

EVALUATION OF SUPERCONDUCTING CHARACTERISTICS ON THE THIN-FILM STRUCTURE BY NbN AND INSULATOR COATINGS ON PURE Nb SUBSTRATE

R. Katayama*, Y. Iwashita, H. Tongu (Kyoto ICR, Uji, Kyoto),
A. Four (CEA/DRF/IRFU, Gif-sur-Yvette), C. Z. Antoine (CEA/IRFU, Gif-sur-Yvette),
H. Hayano, T. Kubo, T. Saeki (KEK, Ibaraki), Hayato Ito (Sokendai, Ibaraki),
R. Ito, T. Nagata (ULVAC, Inc, Chiba),
H. Oikawa (Utsunomiya University, Tochigi)

Abstract

In recent years, it is pointed out that the maximum accelerating gradient of a superconducting RF cavity can be pushed up by coating the inner surface of cavity with a multilayer thin-film structure that consists of alternate insulator and superconductive layers. In this structure, the principal parameter that limits the performance of the cavity is the critical magnetic field or effective Hc1 at which vortices start penetrate into the first superconductor layer. We made a sample that has NbN/SiO2 thin-film structure on pure Nb substrate by DC magnetron sputtering method. In this paper, we will report the measurement results of effective Hc1 of the sample by the third-harmonic voltage method.

INTRODUCTION

Recently, it is pointed out that the effective Hc1 of a superconducting RF cavity might be pushed up by coating the inner surface of cavity with thin-film structure [1–3]. It is known that the effective Hc1 of multi-layer sample is evaluated by detecting the third-harmonic voltage [4]. In the past, C. Antoine showed that a multilayer structure on a Nb substrate has higher effective Hc1 than that of the Nb substrate [5]. We prepared a sample with a multilayer thin-film structure of NbN (200 nm) and SiO2 (30 nm) coated on pure Nb substrate that has the RRR of >250. This article describes details of the measurement of effective Hc1 of the thin-film sample.

THIRD HARMONIC MEASUREMENT

In this section, we briefly explain the measurement setup, measurement flow and procedures, and signal definition used in our third harmonic measurement, though the details of the system is found in elsewhere [6, 7].

Measurement Setup

The sample is held between two copper plates and fixed inside the cryostat. Each copper plates has a tab partially dipped in liquid helium stored at the bottom of the cryostat. As a result, the temperature of the sample is kept at a cryogenic temperature. In the upper copper plate, a coil for applying a magnetic field to the sample is embedded and six zircon balls of 3 mm in diameter sticking out by 200 micrometers from the surface is also embedded to guarantee the distance between the sample and the coil. In the lower copper plate, a heater to raise the temperature of the sample is installed. According to a measurement with a hall probe, it is confirmed that the environmental magnetic field in the cryostat is 0.1 mT or less.

Measurement Flow and Procedure

While applying heat and alternating magnetic field to the sample, current flow and voltage induced in the coil are measured with four-terminal method. The temperatures of both plates are also measured by CERNOX sensors and that of the bottom plate is considered as the sample temperature. The current value is read out as the voltage value generated across the 50 mΩ resistor, while the voltage value induced in the coil is read out after passing it through a high pass filter. Both signals are sampled and converted at 250 ksps to 20-bit digital data and the third harmonic components obtained through Fourier transformations are recorded. In this study, the impedance, calculated from the fundamental component of the coil current and the 3rd order component of the induced coil voltage, is used as the resulted value of the third-harmonic measurement. Finally, the temperature dependence of effective Hc1 is evaluated from both the applied magnetic field and the temperature measured at the moment when a third harmonic signal arises.

Third Harmonic Signal Definition Used in This Study

In this study, the applied magnetic field is recorded as the fundamental component of the coil current. The coil magnetic field is calibrated through a third-harmonic measurement of bulk pure Nb (RRR>250) assuming the following function $F(T)$ is the temperature dependence of effective Hc1 of bulk pure Nb:

$$F(T) = \begin{cases} 0.18 \times \left(1 - (T/9.2)^2\right) & (T < 9.2\text{K}) \\ 0 & (T > 9.2\text{K}) \end{cases} \quad (1)$$

The calibration line obtained by this method is shown in Fig.1. The horizontal axis is the fundamental component of the coil current, and the vertical axis is the coil magnetic field.

* katayama@kyticr.kuicr.kyoto-u.ac.jp

ISBN: 978-3-95450-184-7 doi:10.18429/JACoW-IPAC2018-THPAL015

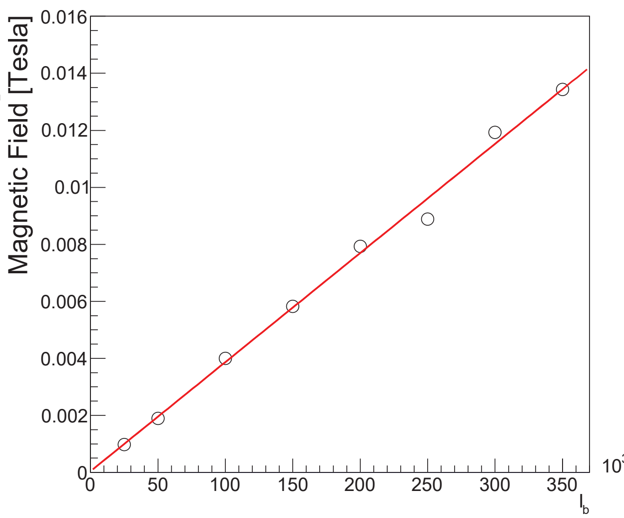

Figure 1: Calibration line of the applied magnetic field vs. the fundamental component of the coil current read I_b (arbitrary unit).

DETAILS OF MEASUREMENT RESULT

The bulk pure Nb substrate of sample is treated in the standard electropolishing recipe for bulk Nb cavity. The thin-film structure of 200-nm NbN and 30-nm SiO2 is created by DC magnetron sputtering on the bulk pure Nb. This sample is named as 180409-1-B, where the details of thin-film creation is found elsewhere [8].

In the third harmonic measurements of this NbN/SiO2/Nb sample, the temperature rising rates were chosen to be about 0.01 K/min. The magnetic field applied to the sample was chosen to be 2.0 mT, 3.8 mT, 5.8 mT, 9.7 mT, and 13.4 mT.

The systematic error in the measured temperature due to a thermal non-uniformity is estimated as follows. At a magnetic field, H, the third harmonic signal vanishes when the temperature is higher than a certain temperature, $T(H)$. In general, when a very weak magnetic field is used, $T(H)$ converges to the critical temperature, T_c. This characteristic indicates that systematic error due to thermal non-uniformity can be determined by the deviation in the measurements of the critical temperature of a sample. Therefore, in this research, third harmonic measurement of bulk pure Nb using a weak magnetic field of 1 mT and 4 mT was performed, and 0.01 K was obtained as the estimated value of the systematic error.

A comparison of third harmonic signals for five different coil magnetic fields is shown in Fig.2. The horizontal axis is the temperature, and the vertical axis is the third harmonic signal. The symbol of H_{app} in the legend denotes the applied magnetic field. In each signal, the sudden rise corresponds to the phase transition, and the temperature dependence of effective Hc1 can be determined. The behavior of signal corresponding to the magnetic field of 2 mT (black plot) is different from other signals. This is because the phase transition of NbN film (black plot) occurs when the bulk pure Nb substrate is in the normal conducting state. On the other hand, the phase transitions of other four signals occur when the bulk pure Nb substrate is in the superconducting state. In this analysis, the temperature at which the third harmonic signal becomes minimum was regarded as the temperature at which the phase transition occurs.

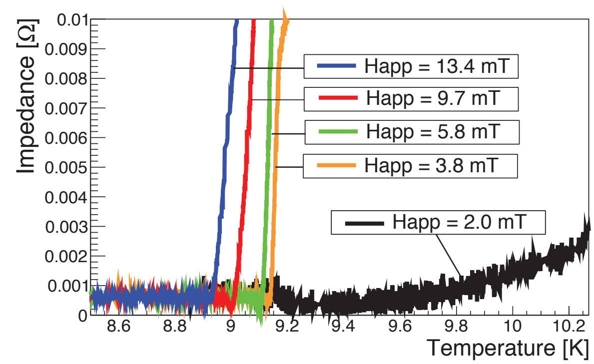

Figure 2: Comparison of the third harmonic signals of NbN/SiO2/Nb. The horizontal axis is temperature, and the vertical axis is the third harmonic signal.

In this study, a sample of bulk pure Nb is made from the same production lot as that of the substrate of NbN/SiO2/Nb. This sample is treated in the same electropolishing recipe as the bulk pure Nb substrate of thin-film sample. By comparing the measurement result of bulk pure Nb to that of NbN/SiO2/Nb, we can directly observe the effect of NbN/SiO2 film. Figure 3 shows the comparison of the third harmonic signals between samples of bulk pure Nb and NbN/SiO2/Nb. The vertical axis is the third harmonic signal, and the horizontal axis is the temperature. In this plot, the applied magnetic field is 13.4 mT. It shows that signals arise at two different temperatures. This difference of the phase transitions is coming only from the effect of NbN/SiO2 film.

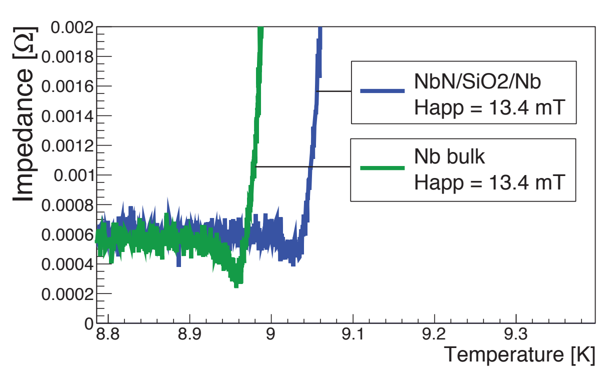

Figure 3: Comparison between third harmonic signals of NbN/SiO2/Nb and bulk pure Nb. Blue plot represents the measurement result for NbN/SiO2/Nb, and green plot represents the measurement result of bulk pure Nb.

ISBN: 978-3-95450-184-7 doi:10.18429/JACoW-IPAC2018-THPAL015

Finally, compiling all data, the temperature dependence of the effective Hc1 of NbN/SiO2/Nb and bulk pure Nb is shown in Fig. 4. The horizontal axis is the temperature, and the vertical axis is the measured effective Hc1. The open circle is the measurement result of Hc1 of bulk pure Nb sample, and the black triangle is the measurement result of effective Hc1 of NbN/SiO2/Nb sample. The red curve is the equation (1) which is used for the calibration. The green dashed curve is obtained by fitting data points of thin-film sample in the region of T<9.2 K with the function of (2), and the blue chain curve is obtained by fitting data points of thin-film sample in the region of T>9.2 K with the function of (2). The fitting of blue chain curve includes the measured Tc of 13.8 K for NbN/SiO2/Nb sample (sample No.180409-1-A) [9]. It is clearly confirmed that the effective Hc1 is improved by the NbN/SiO2 film. These results are thought to be the evidence that the magnetic field reaching the Nb substrate is partially shielded by the NbN/SiO2 film. At the temperature greater than around 9.2 K, the effective Hc1 is determined by the blue chain curve due to only NbN film in superconducting state, whereas at the temperature below around 9.2 K, the effective Hc1 is determined by the green dashed curve due to the whole NbN/SiO2/Nb structure in the superconducting state. As a result of fitting, $f(0)$ and Tc', parameters of the function (2), are determined as 0.219 and 9.22 for green dashed curve, whereas $f(0)$ and Tc' are determined as 0.004 and 13.78 for blue chain curve.

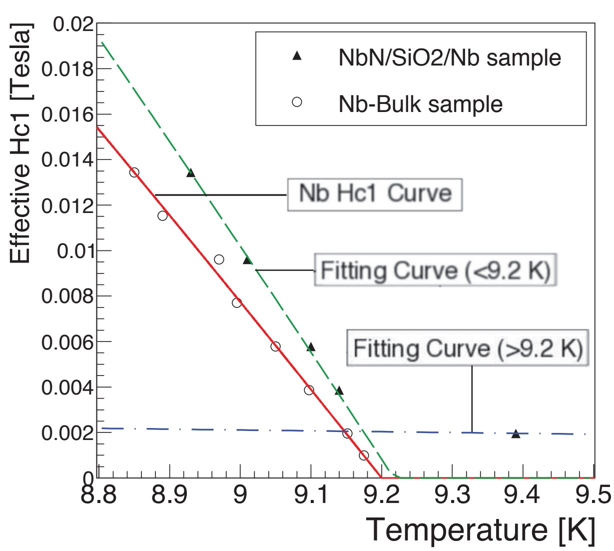

Figure 4: Comparison of measured effective Hc1 between NbN/SiO2/Nb and bulk pure Nb samples. The red curve is the equation (1) which is used for the calibration. The green dashed and blue chain curves are obtained by fitting data points of NbN/SiO2/Nb sample.

SUMMARY AND FUTURE PROSPECT

We evaluated the temperature dependence of effective Hc1 of multi-layer thin-film sample consisting of NbN superconductive layer (200 nm) and SiO2 insulator layer (30 nm) formed on bulk pure Nb. This study is the first case that multi-layer thin-film formed on pure Nb bulk substrate which has RRR>250 is evaluated with the third harmonic measurement. The measurement result clearly showed that the effective Hc1 of bulk pure Nb was improved by NbN/SiO2 film coating. As a future prospect, we would like to evaluate effective Hc1 using a stronger magnetic field in lower temperature region. In addition, we would like to clarify the temperature dependences of various multilayered thin film samples with different thickness and the number of layers.

ACKNOWLEDGEMENTS

This work is supported by JSPS KAKENHI Grant Number JP17H04839, JSPS KAKENHI Grant Number JP26600142, Photon and Quantum Basic Research Coordinated Development Program of MEXT, Japan, Center of Innovation (COI) Program, Japan-US Research Collaboration Program, and the Collaborative Research Program of Institute for Chemical Research, Kyoto University (2016-8).

APPENDIX

In this paper, the following function is used in Fig. 4:

$$f(T) \quad = \quad f(0) \times \left(1 - (T/T_c')^2\right) \qquad (2)$$

REFERENCES

[1] A. Gurevich, "Enhancement of rf breakdown field of superconductors by multilayer coating", Appl. Phys. Lett. 88, 012511 (2006).

[2] T. Kubo, *et al.*, "Radio-frequency electromagnetic field and vortex penetration in multi-layered super-conductors", Appl. Phys. Lett. 104, 032603 (2014).

[3] T. Kubo, "Multilayer coating for higher accelerating fields in superconducting radio-frequency cavities: a review of theoretical aspects", Supercond. Sci. Tech-nol. 30, 023001 (2017).

[4] G. Lamura, M. Aurino, A. Andreone, and J.-C. Villégier, "First critical field measurements of superconducting films by third harmonic analysis", J. Appl. Phys.106, 053903 (2009).

[5] C. Z. Antoine, M. Aburas, A. Four, *et al.*, "Progress on characterization and optimization of multilayers", SRF2017 Proceedings, Lanzhou, China.

[6] Y. Iwashita, H. Tongu, H. Hayano, *et al.*, "Measurement of Thin Film Coating on Superconductors", Proceedings of IPAC2017, Copenhagen, Denmark.

[7] Y. Iwashita, H. Tongu, H. Hayano, *et al.*, "R&D of Thin Film Coating on Superconductors", SRF2017 Proceedings, Lanzhou, China.

[8] R. Ito, T. Nagata, *et al.*, "Development of Coating Technique for Superconducting Multilayered Structure", IPAC2018 Proceedings, Vancouver, Canada, April-May 2018.

[9] H. Ito, *et al.*, "Lower Critical Field Measurement System of Thin Film Superconductor", Presented at IPAC2018, Vancouver, Canada, April-May 2018.